ASTFE
American Society
of Thermal and Fluids Engineers

5th Thermal and Fluids Engineering Conference (TFEC)
April 5–8, 2020
New Orleans, LA, USA

TFEC-2020-31803

A MANY-BODY DISSIPATIVE PARTICLE DYNAMICS STUDY OF COALESCENCE INDUCED JUMPING

Ting Liu[1†], Anupam Mishra[1], Ahmed A. Hemeda[1], James Palko[1], and Yanbao Ma[1*]

[1]University of California, Merced, California 95343, United States

ABSTRACT

Coalescence induced jumping from solid surface at mesoscale is simulated using Many-body dissipative particle dynamics (MDPD). The geometrical evolution during the coalescence of two droplets and resulted jumping were obtained and the mechanism behind this phenomenon were also investigated. The jumping maps two equal-sized droplets and two droplets with different sizes were obtained. It is found the coalescence of two equal size droplets will lead to jumping when the contact angle is larger than the minimum threshold contact angle, which is about 160°. This minimum threshold contact angle is related to droplet size as it increases when droplet size decreases. Jumping can still happen when two droplets with different sizes merge together. The maximum volume ratio for jumping of two droplets with different sizes is 3.9. Velocity field shows how internal flow evolves during the coalescence process. There is obvious velocity change inside the droplet from the beginning of the droplet deformation to jumping. The energy conversion rate from released surface energy to kinetic energy is found about 1%. These results can greatly advance the fundamental understanding of hydrodynamics behavior of coalescence induced droplet jumping.

KEY WORDS: MDPD, Coalescence, Jumping, Contact angle, Velocity fields

1. INTRODUCTION

Coalescence-induced droplet jumping on a superhydrophobic surface was first reported by Boreyko and Chen [1]. Since then this phenomenon has been intensively investigated through experimental measurement [2] [3] [4], theoretical analysis [5] [6] [7] and numerical simulations [8] [9] [10] [11] as it aroused wide range of academic interest and industrial applications in fields such as condensation heat transfer enhancement [12] [13], self-cleaning [14] [15], anti-icing [16] [17] , anti-corrosion [18] [19] and energy harvesting [20].

By the way of experimental approach, Chen et al. [2] systematically investigated the jumping height of condensate droplets jump from the hierarchical superhydrophobic surfaces having truncated microcones coated with nanostructures and found droplet jumping height increases with a decrease in microcone pitch. Chen et al. [3] observed coalescence induced jumping of multiple condensate droplets on hierarchical superhydrophobic surfaces and found the highest jumping velocity was achieved when two droplets coalesce. By using a combination of side-view and top-view high-speed imaging, Kim et al. [4] found three fundamentally different droplet jumping mechanisms: (1) coalescence of two neighboring droplets, (2) coalescence of multiple droplets, and (3) coalescence between droplets on the surface and a returning droplet that has already departed. Among these investigations, coalescence induced jumping was visually observed from micrometer to millimeter scale.

For theoretical analysis, Wang et al. [5] presented analysis based on the energy conservation for the coalescence of two droplets of the same size on a superhydrophobic rough surface and reveals that the

*Corresponding Author: yma5@ucmerced.edu
†Speaker

coalescence induced jumping can only occur with the droplet radius ranging from several microns to a few millimeters. Nam et al. [6] conducted energy and hydrodynamic analyses of coalescence-induced jumping on superhydrophobic surfaces by developing a full 3D unsteady model based on the level contour reconstruction method and investigated the dynamic changes in surface energy, kinetic energy, potential energy and viscous energy during the droplet evolution period. Cha et al. [7] stated the combined effects of adhesion, contact angle hysteresis, and initial wetting behavior governed by the surface structure morphology and length scale play a defining role on coalescence induced jumping.

Regarding numerical simulations, Peng et al. [8] investigated the dynamic evolution of droplet and the velocity distribution inside the droplet during coalescence using multiphase lattice Boltzmann method. Vahabi et al. [9] applied volume of fluid method and demonstrated coalescence-induced jumping with an energy conversion efficiency of 18.8% on a superhydrophobic surfaces with a macrotexture comparable to the droplet size. Gao et al. [10] found that attraction force between the surface and water molecules is critical to the coalescence process of two equally sized nanodroplets by molecular dynamics simulation. Zhang et al. [11] employed many-body dissipative particle dynamics to investigate the wetting behavior of an isolated droplet and coalescence of droplets for both Cassie-Baxter and Wenzel states.

Although people have thoroughly investigated this phenomenon, current understanding of coalescence induced droplet jumping is still hindered by limited properly modeling detailed transient behaviors of this rapid and complex shape change processes. From these previous studies, coalescence induced jumping was experimentally observed from micrometer to millimeter scale and simulated from nanometer to micrometer scale. Therefore, simulation methods for micrometer scale (mesoscale) is a better choice to obtain in-depth insights into the dynamics of coalescence induced droplet jumping to match experimental measurements. In the present study, as a powerful avenue to investigate the characteristics of droplets at different range of time and spatial scales in which many wetting phenomena in nature take place [21] [22] [23], many-body dissipative particle dynamics simulation is constructed for droplet sitting on smoothed hydrophobic surfaces.

The main purpose of this study is to: (1) investigate the jumping conditions for two droplets with same size and different size on superhydrophobic surface in mesoscale; (2) capture the velocity distribution inside the merged droplet during droplets coalescence. Jumping conditions can provide performance prediction and design of current and future superhydrophobic surfaces. Gaining a fundamental understanding of the droplet internal dynamics is crucial to manipulate liquids inside the small droplets.

2. NUMERICAL MODELING

In the present study, coalescence induced droplet jumping dynamics have been simulated by employing MDPD. MDPD is a coarse-grained mesh-free method based on the standard dissipative particle dynamics (DPD) method [24][25][26]. In DPD/MDPD, a group of fluid/solid molecules are incorporated into a soft bead as a coarse-grained particle. Therefore, the simulation scale of DPD/MDPD approaches is much larger than molecular dynamics (MD), lying in a meso-scale regime which is between the atomic and continumm scales [27][28]. Hence the simulation time can be significantly reduced. It has been proved that the computational cost is 20 times lower for DPD or MDPD to achieve the same real time compared to MD [29]. Another advantage is MDPD utilizes soft interaction potential rather than conventional Lennard-Jones interactions, which enables it to capture complex physics to study the dynamics of fluid-structure interactions. By employing a correct description of hydrodynamic interactions and a thermostat capable of conserving local momentum, MDPD can simulate isothermal fluid system in a fully isotropic and Galilean invariant manner with larger time scales.

2.1 Governing Equations

In MDPD simulation, each particle is characterized by its location $\vec{r}$, velocity $\vec{v}_i$, and its mass m_i. The motion of the i^{th} particle with unit mass is determined by Newton's second law:

$$\frac{d\vec{r}_i}{dt} = \vec{v}_i \tag{1}$$

$$m_i \frac{d\vec{v}_i}{dt} = \vec{f}_i = \sum_{j \neq i} (\vec{f}_{ij}^{\,C} + \vec{f}_{ij}^{\,D} + \vec{f}_{ij}^{\,R}) + \vec{F}_b \tag{2}$$

where $\vec{f}$ is the total force that exerts on a single particle, which can be categorized into three different classes: conservative force $\vec{f}_{ij}^{\,C}$, dissipative force $\vec{f}_{ij}^{\,D}$ and random force $\vec{f}_{ij}^{\,R}$. The external body force exerted on each bead is incorporated into the model by parameter $\vec{F}_b$. Note that all the forces' contributions in MDPD are pairwise. The force components of each particle pair can be expressed as [30]:

$$\vec{f}_{ij}^{\,C} = A_{ij}\omega_C(r_{ij}, R_c)\vec{e}_{ij} + B_{ij}(\bar{\rho}_i + \bar{\rho}_j)\omega_C(r_{ij}, R_d) \tag{3}$$

$$\vec{f}_{ij}^{\,D} = -\gamma\omega_D(r_{ij}, R_c)(\vec{e}_{ij} \cdot \vec{v}_{ij})\vec{e}_{ij} \tag{4}$$

$$\vec{f}_{ij}^{\,R} = \varphi\omega_R(r_{ij}, R_c)\theta_{ij}\Delta t^{-\frac{1}{2}}\vec{e}_{ij} \tag{5}$$

where $r_{ij} = |\vec{r}_{ij}|$, $\vec{r}_{ij} = \vec{r}_i - \vec{r}_j$, $\vec{e}_{ij} = \vec{r}_{ij} / |\vec{r}_{ij}|$ and $\vec{v}_{ij} = \vec{v}_i - \vec{v}_j$.

For the conservative force, A_{ij} and B_{ij} denote the maximum attractive and repulsive force amplitudes among particles i and j respectively, where i and j can be vapor v, liquid l and solid s. ω_C is the weighting function ω_C vanishing when r is larger than cut-off radius R_c. The weighting function is defined by $\omega_C(r_{ij}, R_c) = \max(1 - r_{ij}/R_c, 0)$. R_d is a secondary cutoff radius specifically defined for MDPD and usually considered as $0.75R_c$. Noting that Warren proposed the density-dependent conservative force formula empirically with this secondary cut-off range R_d, the local density for each particle is given with the shape of [24]:

$$\vec{\rho}_i = \sum_{j \neq i} \frac{15}{2\pi R_d^3}\left(1 - \frac{r_{ij}}{R_d}\right)^2 \tag{6}$$

For dissipative and random force, the parameters γ and φ are the dissipative and random force amplitudes, respectively. The parameter θ_{ij} is the Gaussian white noise with zero mean and unit variance, and Δt is the time step. The relationship between random and dissipative weighting functions is governed by $\omega_D(r_{ij}, R_c) = [\omega_R(r_{ij}, R_c)]^2 = \max(1 - r_{ij}/R_d, 0)$, and $\gamma = \varphi^2 / 2k_B T$, where k_B is the Boltzmann constant and T is the temperature of the system. Hence, a thermostat is established preserving the momentum and regulating the temperature. The random force in the model reveal the effect of Brownian motion of particles.

2.2 Fluid/Structure Interaction

In MDPD simulation, although wall/solid particles are assumed to be frozen for simplification [31][32], they still have active interaction with fluid particles. As all three forces components between DPD particles are short-range interactions, large time steps can be realized for the interaction between particles within the domain. However, fluid particles would be able to penetrate into wall/solid particles because the soft interaction between DPD particles unlike the hard potentials in molecular dynamics. Hence, boundary condition at the fluid-solid interfaces should be specially considered to avoid this problem [33]. In this study, bounce-back boundary condition was implemented to prevent penetration of fluid particles into solid particles and make them adhere to the no-slip boundary condition. The bounce-back boundary condition on a flat wall can be written as:

$$\vec{v}_{i,m} = \vec{v}_{i,p} \tag{7}$$

$$\vec{r}_{i,m} = 2\tau(\vec{r}_{i,o} - \vec{r}_{i,p}) + \vec{r}_{i,p} \tag{8}$$

where, $\tau = (Z_s - Z_p)/(Z_o - Z_p)$ and subscripts m, o, p and s denote modified, old, predicted and solid wall respectively. Z is the vertical component of $\vec{r}$ to calculate parameter τ.

Table 1. Parameter values in MDPD simulation

Parameter	Symbol	DPD Value	Physical value
Particle mass	m	1.0	
System energy	k_BT	1.0	
Cut-off radius of attractive force	R_c	1.0	
Cut-off radius of repulsive force	R_d	0.75	
Attraction parameter (liquid-liquid)	A_{ll}	-40	
Repulsion parameter	B_{ll}	25	
Amplitude of random force	φ	6.0	
Time step	Δt	0.01	
Fluid particle density	ρ	6.10	998 kg/m^3
Liquid-vapor surface tension	σ	7.30	0.072N/m
Liquid dynamic viscosity	ν	7.45	1.0×10^{-6} m^2/s

In the model, the interaction of solid and fluid particles is represented by the repulsion force amplitude in the conservative force between them, which is A_{sl} [34]. Hence, A_{sl} is the only interaction parameter needs to be modified to change the interaction of solid and fluid particles for different static or dynamic behavior, while the rest of the interaction parameters remain the same constant. The values of used parameters in this study are presented in Table 1.

2.3. Dimensional Analysis

MDPD is a coarse graining method using dimensionless unit system. To calculate hydro-physical properties of MDPD simulation, specific transformation need be performed to compare the MDPD simulation geometry with physical units. Taking the fluid density, kinematic viscosity and surface tensions in MDPD unit as d, ν and σ, in SI unit as d^*, $\nu*$ and $\sigma*$, respectively, the physical length, mass and time of MDPD are obtained using the following formula [32]:

$$L_{DPD} = \frac{d^*}{d}\left(\frac{\nu*}{\nu}\right)\frac{\sigma}{\sigma*} \tag{9}$$

$$T_{DPD} = L^2{}_{DPD}\,\frac{\nu}{\nu*} \tag{10}$$

$$M_{DPD} = \frac{d^*}{d}L^3{}_{DPD} \tag{11}$$

By taking water as the fluid phase in the simulation with properties and the corresponding values in the DPD units in Table 1, DPD unit length can be calculated as follow:

$$L_{DPD} = \frac{998kg/m^3}{6.1} \times \left(\frac{1.0\times10^{-6} m^2/s}{7.45/6.1} \right)^2 \times \frac{7.3}{0.072N/m}$$

This gives $L_{DPD} \approx 1.1\times10^{-8} m$ for the unit length in DPD compared with the physical domain. Time and mass are calculated in Table 2. These values are significantly larger compared with the unit values in MD simulations [35]. All subsequent simulation results including energy, time and length in this study are based on DPD units, the physical units of these findings can be calculated based on the results in Table. 2. For example, simulations are performed in a three-dimensional computational region of size 100×100×100 in DPD unit, which is about 1.1 μm×1.1 μm×1.1 μm in physics unit.

Table 2. DPD units and their equivalent in SI unit.

Parameter	DPD Unit Symbol	SI
Length	L_{DPD}	1.1×10^{-8} m
Time	T_{DPD}	1.3×10^{-10} s
Mass	M_{DPD}	1.63×10^{-22} kg

3. COALESCENCE INDUCED JUMPING SIMULATION

In this study, wettability of solid surface is an important factor to the jumping phenomenon. In MDPD simulation, wettability can be changed by modifying the attractive component in conservative force. To formulate the wettability as a function of A_{sl}, the static contact angle of a sessile droplet sitting on a flat wall is calculated for various A_{sl} values. The relationship of A_{sl} and the static contact angle of a droplet on a flat substrate has good match with previous studies by Chen [36], Chang [37], and Zhang [11].

In this section, droplet detachment from a surface induced by the coalescence of two droplet is investigated. It is known that with hydrophilic surface, water droplet extend itself on surface with larger water-gas interface compared to hydrophobic surface. Therefore, if the droplet is going to detach from the surface without external force, the surface must be hydrophobic surface. Furthermore, superhydrophobic surfaces provide the effective energy conversion from the surface energy to the kinetic energy and improve the reproducibility of the droplet jumping. To mimic this process, two droplets with same three phase contact angle are created and sit on a hydrophobic substrate next to each other, as shown in the Fig. 1.

Although the two droplets are in static condition from the beginning, with the effect of random force in MDPD simulation scheme, the particles will move around randomly inside the droplets. Therefore, the shape of the droplets will no longer be exactly a sphere cap but will changing its shape slightly. As a result, particles in one droplet will meet particles in the other droplet and leading to the coalescence of two droplet. While the coalescence occurred in all cases, depending on the radius of the droplets, and initial three phase contact angle on the surface, the final coalesced droplet may or may not jump off and detach from the surface.

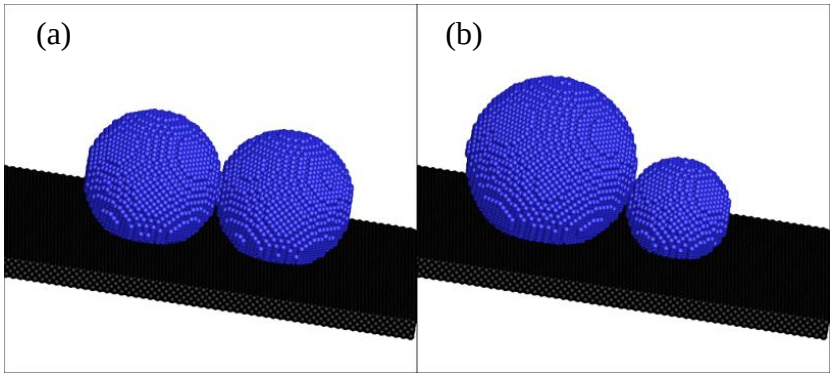

Fig. 1. Coalescence Induced Jumping Simulation Set-up: (a) Droplets with same size; (b) with different size.

4. RESULTS AND DISCUSSION

4.1. Jumping Conditions Analysis

After the coalescence induced jumping simulation set-up, by testing a wide range of A_{sl} values, i.e. contact angle of the droplet, the jumping map is obtained for two droplets with same radius from 6 to 11 in DPD unit length, shown in Fig. 2. These radii are associated with particle numbers 10,688, 16,980, 25,290, 36,094, 49,458 and 65,822 for two droplets, respectively.

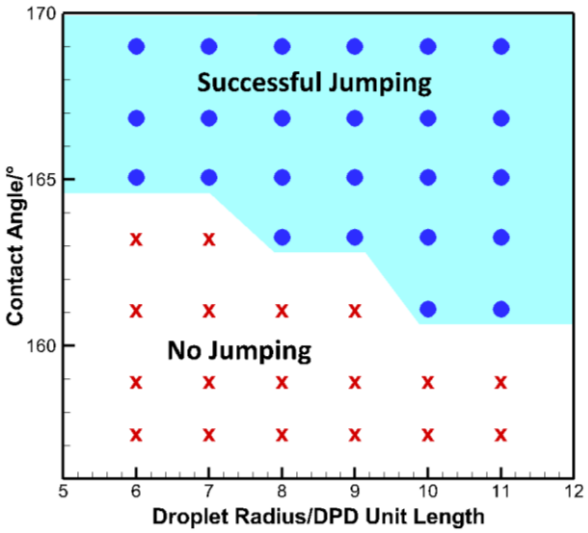

Fig. 2. Droplets with same size electro-wettability jumping map

For droplets with same size, from Fig. 2, it can be found that the threshold contact angle for a coalesced droplet to jump decreased with larger radius, while the minimum threshold contact angle for jumping is 161° when radius is 11 in DPD unit length. Therefore, when the contact angle is larger than the maximum threshold contact angle, the coalescence of two equal size droplets will lead to jumping.

How about if the two droplets are of different size? To answer this question, plenty of cases with contact angle 165° were tested and the jumping map for droplets with same contact angle but different size is in Fig. 3. From the figure, jumping can still happen when two droplets with different size merge together. However, there is a maximum size difference for jumping between the two droplets. This size difference increases when droplet radius is larger.

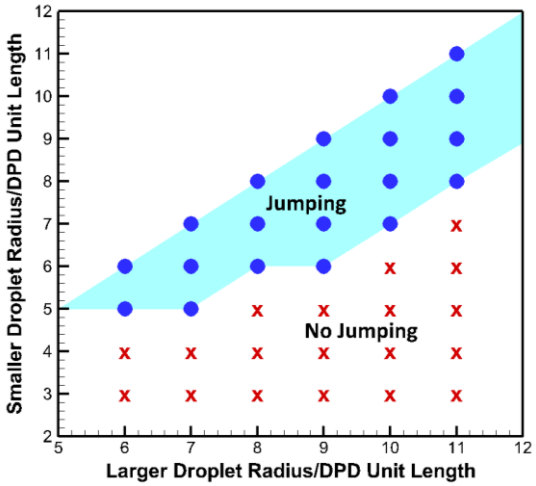

Fig. 3. Droplets with different size electro-wettability jumping map

These findings can be explained from energy aspect. It is known that the kinetic energy for jumping comes from the release of surface energy when the coalescence happens, although people showed different results in this energy conversion efficiency [9] [6] [38] [39]. Total surface free energy is the sum of liquid-vapor surface energy and liquid-solid surface energy, which is defined as:

$$E_s = A_{ls}\sigma_{ls} + A_{lv}\sigma_{lv} \tag{12}$$

where σ_{ls} and σ_{lv} are interfacial tension of liquid-solid interface and liquid-vapor interface respectively. According to Young's Equation:

$$\sigma_{ls} = \sigma_{sv} - \sigma_{lv}\cos\theta \tag{13}$$

where θ is the contact angle of the liquid phase and σ_{sv} is the solid-vapor interfacial tension. However, σ_{sv} can be considered as 0 when there is no vapor particles[40]. Then we have:

$$\sigma_{ls} = -\sigma_{lv}\cos\theta \tag{14}$$

where the negative sign only indicates the direction of interfacial tension. Therefore, the total surface free energy can be written as:

$$E_s = \sigma_{lv}(A_{ls}|\cos\theta| + A_{lv}) \tag{15}$$

Hence, for larger droplets, they possess larger surface area and higher surface energy potential. More energy could be released and converted to kinetic energy and make the droplet to jump from the solid substrate. For smaller droplets to have the same surface energy potential with lager droplets, the contact angle should be larger. This explains why the threshold contact angle for jumping is smaller for larger droplets and minimum size difference for jumping increases with lager droplets when two droplets are not the equal size.

4.2. Coalescence of Two Equal-sized Droplets

For those successful jumping cases, the evolution process of different stages of coalescence induced jumping for two equal-sized droplets are illustrated in Fig. 4. To better visualize this process, the two droplets are marked in different colour. From the figure, there are four stages for the coalescence induced jumping process [10] [41]: (i) formation and growth of the liquid bridge of the merged droplet. A peanut shape droplet was formed in the early stage of coalescence when surface fluid particles in the original two droplets met each other. (ii) impact of the liquid bridge on the surface. The radius of the liquid bridge grows and finally contact with the surface. (iii) reduction of the liquid solid interface area. Under the effect of surface tension which has the potential to maintain minimum surface area, more fluids particles in the original two droplets moved to the centre to reduce the surface area and a sphere cap shape droplet was formed. (iv) upward motion and jumping of droplet. With the release of surface energy as a result of reduced surface energy, the mass centre of the droplet grows higher and the droplet finally jumped from the solid substrate.

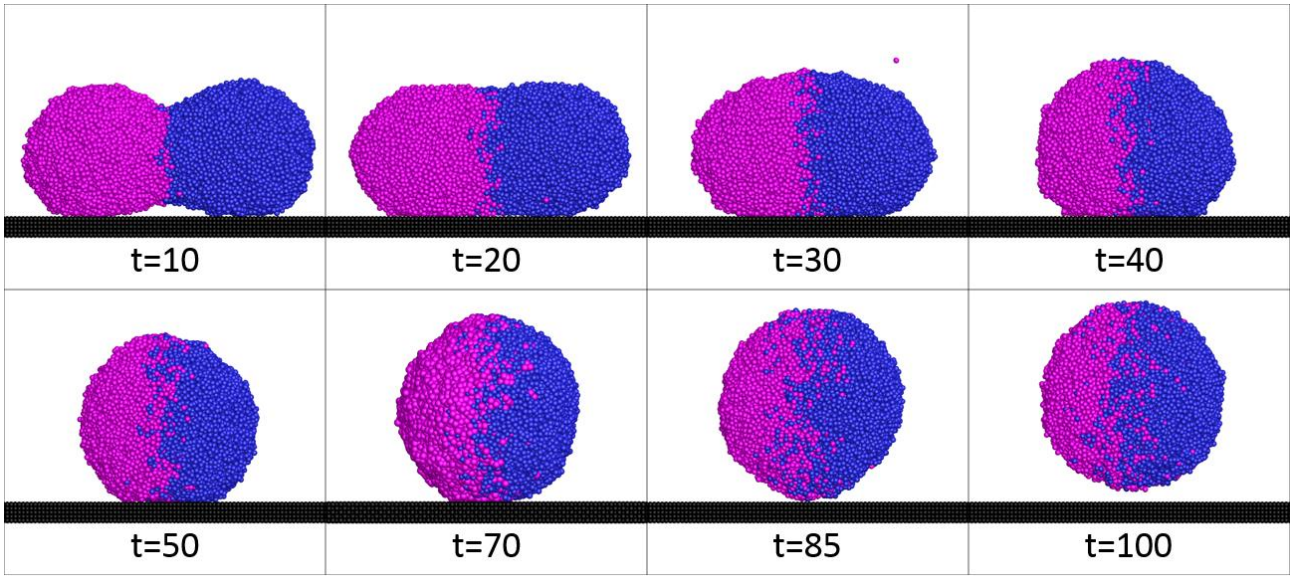

Fig. 4. Various stages of coalescence induced jumping of two equal-sized droplets/DPD unit time.

To better understand the process of coalescence induced jumping, the internal flow field of the merged droplet was examined. Note that there are thermal fluctuation and Brownian motion in MDPD simulation, the velocity field of each particle at any moment has random contribution and fluctuation. Averaging method should be applied here to eliminate this effect and obtain statistically steady local velocity vectors. Therefore, the computational domain is divided into cubical cells. Then the local velocities are obtained by adding and averaging the sampled data over sufficient time steps at each cubic cell to eliminate the effect of randomness.

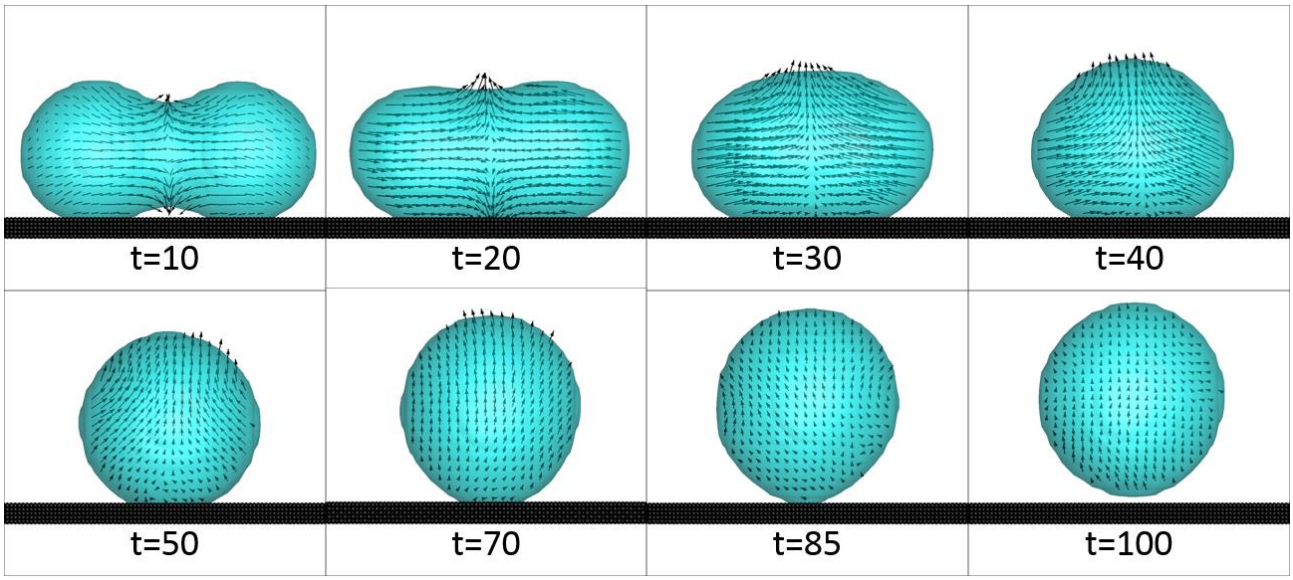

Fig. 5. Velocity distribution for various stages of two equal-sized droplets /DPD unit time.

Velocity distribution within the merged droplet due to coalescence for various stages are shown in Fig. 5. Velocity vectors were plotted with their relative length. From Fig. 5, velocity vectors concentrate on the junction part of the peanut shape droplet at the beginning of the coalescence, while particles in both sides kept almost static. Then with the dragging of the particles moving to centre, particles in both sides began moving toward droplet centre and formed a capsule shape droplet. Under the effect of surface tension, more particles move to droplet centre, the capsule shape droplet converted into a sphere cap shape. In this process,

plenty of surface energy was released and converted into kinetic energy as a result of decreased surface area. This resulted the obvious velocity vectors length increase at t=30. As particles from both sides continue moving to droplet centre, the droplet centre was fully occupied and droplet particles need to go away from centre. Like the collision of two moving droplets, particle will disperse in the collision interface. However, there is a solid substrate in this case. Together with the effect of surface tension, those particles can only move upward. During this fast collision process, plenty of kinetic energy was dissipated and the directions of velocity vectors changed from horizontal to vertical, which were cleared shown from t=40 to t=50. With the rest kinetic energy, the droplet then jumped from the substrate.

Velocity in coalescence direction and vertical direction is also recorded in Fig. 6. For two equal-sized droplets, horizontal coalescence velocity reaches maximum in the first 2 stages, while vertical velocity reaches minimum as the capillary bridge impinges on solid surface. As the horizontal coalescence velocity is in opposite direction for two droplets, this horizontal coalescence velocity then decreased as two droplets merges more together. Vertical velocity reached maximum when horizontal coalescence velocity decreased to minimum. However, the maximum vertical velocity is reached before jumping. To overcome the adhesion to solid surface, vertical velocity is decreased for jumping.

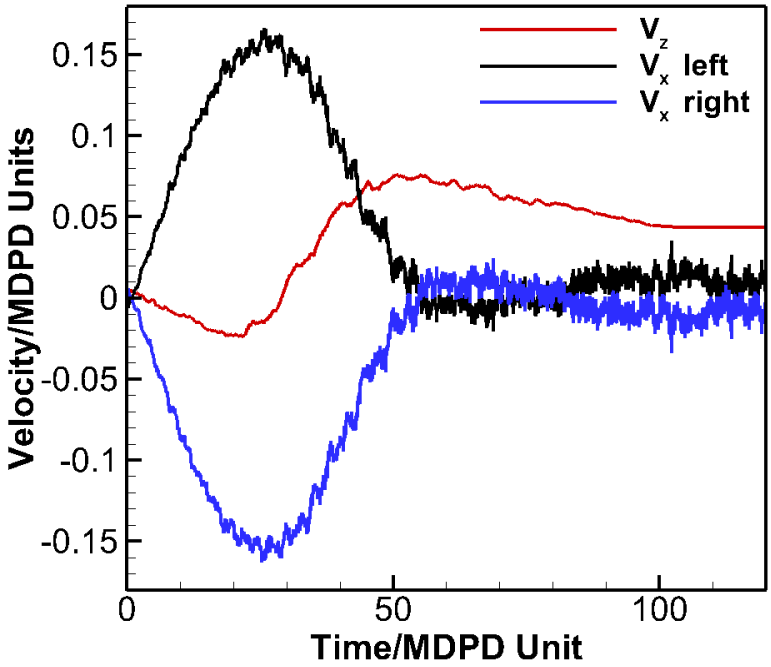

Fig. 6. Horizontal and vertical velocity evolution of two equal-sized droplets /DPD unit time.

4.3. Coalescence of Two Droplets with Different Size

The evolution process of different stages of coalescence induced jumping for two droplets with different size are illustrated in Fig. 7. Similar to the coalescence of two equal-sized droplets, there are also four stages for the coalescence of two droplets with different size.

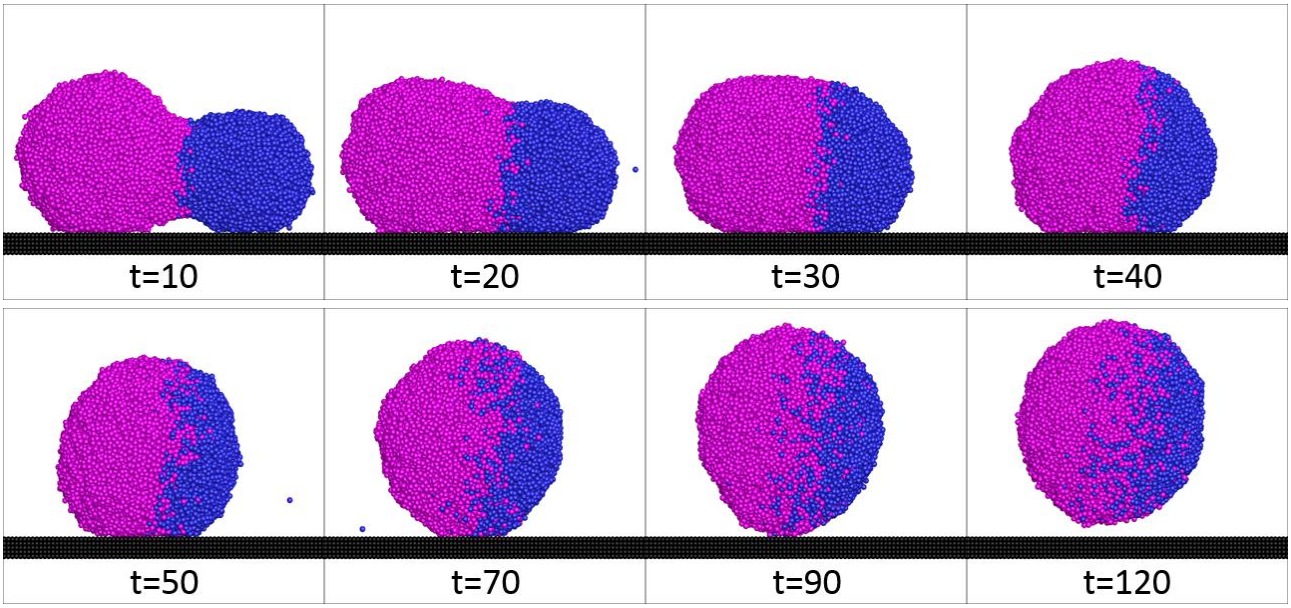

Fig. 7. Various stages of two droplets with different size/DPD unit time.

To compare the of coalescence process of two droplets with different size with two equal-sized droplets, the internal flow field of the merged droplet from two droplets with different size was also examined, as shown in Fig. 8. The internal flow is not symmetric anymore for two droplets with different size.

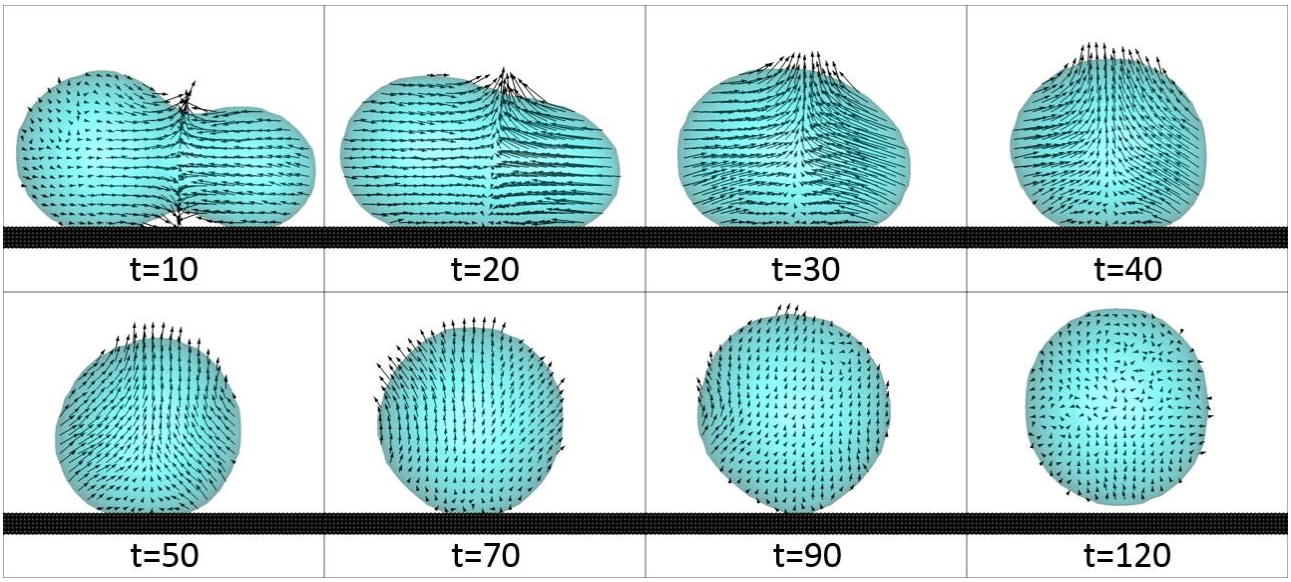

Fig. 8. Velocity distribution for various stages of coalescence induced jumping by two droplets with different size/DPD unit time.

Velocity in coalescence direction and vertical direction is also recorded in Fig. 9. The evolution trend is almost the same to the case of two equal-sized droplets with only one difference. The horizontal velocity is not the same for each droplet as the small droplet has a much larger horizontal coalescence velocity, which can also be seem from t=20 in Fig. 8.

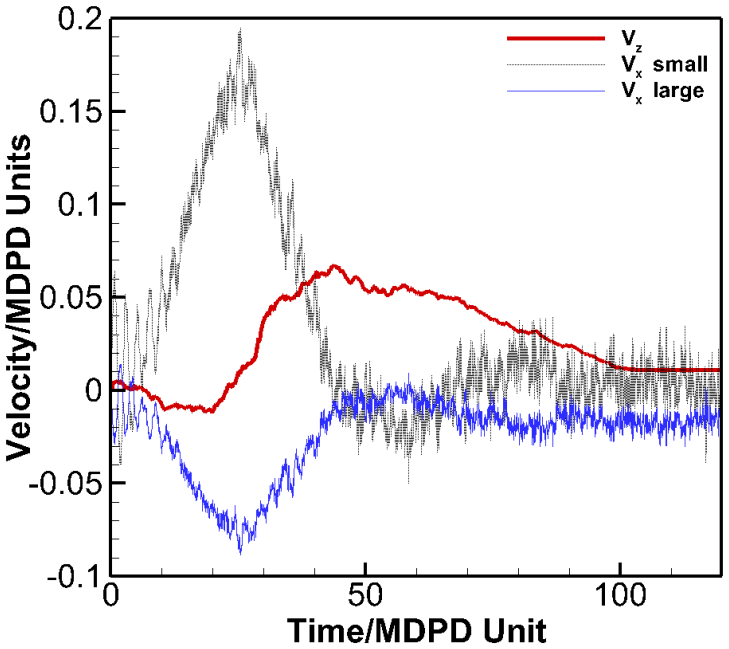

Fig. 9. Horizontal and vertical velocity evolution of two droplets with different size/DPD unit time.

4.4. Energy Analysis

The merged droplet mass center in z-direction versus time was recorded as in Fig. 10. Since it has been discussed above that the physics unit of MDPD simulation is from 10 nanometers to several micrometers, capillary force dominates the movement of droplet particles. Therefore, gravity is not considered in our simulation. From the figure, it can be found that the mass center in z-direction increases very slowly from t=0 to t=30 when particles were mainly moving horizontally toward droplet center. From t=40, the mass center in z-direction increases much faster as particles moving upward to detach from the substrate. This corresponds well with the results from velocity distribution.

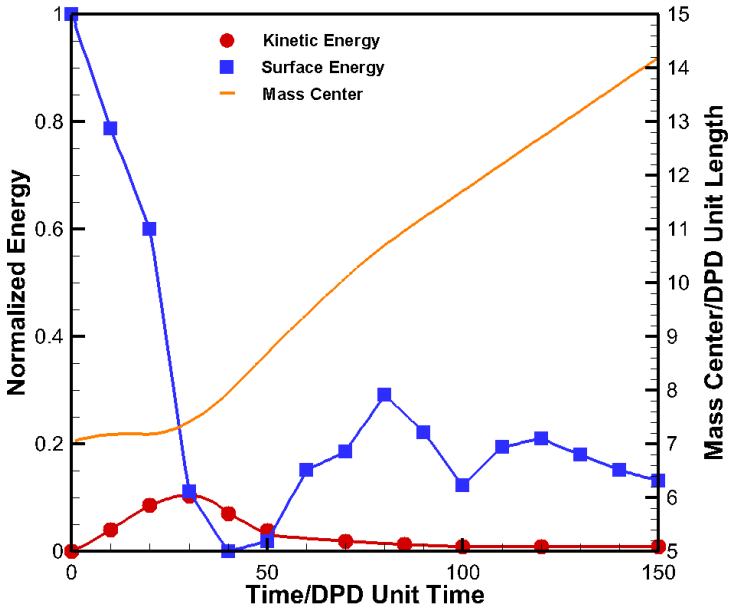

Fig. 10. Energy and mass center vs Time in DPD units

Since the detachment of droplet is the results of surface energy releasing, the evolvement of surface energy and kinetic energy are recorded in our model as shown in Fig. 10, which is similar to previous studies conducted by Cavalli [42] and Islam [43]. Note that only a small portion (only about 1%) of the reduced surface energy converted into kinetic energy as the rest is dissipated because of the viscos dissipation. From the figure, the velocity increased suddenly after the wettability of the substrate is changed as particle move upward and reached its maximum before jumping. As in static condition, even in a superhydrophobic substrate, droplet will sit in the substrate as a part spherical shape. In order to jump from the substrate, part of the kinetic energy is dissipated to overcome the liquid-solid adhesion. Therefore, the velocity then decreased and remains almost constant after it detached from the substrate.

5. CONCLUSIONS

In this study, the MDPD method is successfully used to simulate the dynamic electrowetting-induced droplet jumping process. The geometrical evolution of the jumping droplet induced by electrowetting and the mechanism behind it have been investigated. The electrowetting process is simulated by changing the wettability of solid surface from hydrophilic to superhydrophobic. The contributions of this study include three parts. Firstly, by generating the jumping map, the threshold jumping contact angle for two droplets with same size and the minimum radius difference for two different size droplets with same contact angle were obtained. Second, the present numerical simulations provide additional details of the dynamic velocity field within the merged droplet during the coalescence and jumping process, from which the dynamic geometrical evolution of the droplet and how droplet deform its shape are captured. In the end, various transient energy evolutions are obtained to elucidate the mechanism of coalescence induced droplet jumping. The results obtained in this study not only greatly advance the fundamental understanding of the complex flow physics inside the jumping droplets but also provide a guidance for optimal design of manipulation of droplets in mesoscale.

ACKNOWLEDGMENT

Authors gratefully acknowledges funding support from NSF under grant number CCF #1718194.

REFERENCES

[1] J. B. Boreyko and C. Chen, “Self-Propelled Dropwise Condensate on Superhydrophobic Surfaces,” vol. 184501, no. October, pp. 2–5, 2009.

[2] X. Chen, J. A. Weibel, and S. V Garimella, “Characterization of Coalescence-Induced Droplet Jumping Height on Hierarchical Superhydrophobic Surfaces,” 2017.

[3] X. Chen, R. S. Patel, J. A. Weibel, and S. V. Garimella, “Coalescence-Induced Jumping of Multiple Condensate Droplets on Hierarchical Superhydrophobic Surfaces,” *Sci. Rep.*, vol. 6, no. September 2015, pp. 1–11, 2016.

[4] M. K. Kim *et al.*, “Enhanced Jumping-Droplet Departure,” *Langmuir*, vol. 31, no. 49, pp. 13452–13466, 2015.

[5] F. Wang, F. Yang, and Y. Zhao, “Size effect on the coalescence-induced self-propelled droplet Size effect on the coalescence-induced self-propelled droplet,” no. August 2014, 2011.

[6] Y. Nam, H. Kim, and S. Shin, “Energy and hydrodynamic analyses of coalescence-induced jumping droplets,” vol. 161601, no. 2013, 2016.

[7] H. Cha, C. Xu, J. Sotelo, J. M. Chun, and Y. Yokoyama, “Coalescence-induced nanodroplet jumping,” vol. 064102, pp. 1–18, 2016.

[8] B. Peng, S. Wang, Z. Lan, W. Xu, R. Wen, and X. Ma, “Analysis of droplet jumping phenomenon with lattice Boltzmann simulation of droplet coalescence,” vol. 151601, no. 2013, 2017.

[9] H. Vahabi, W. Wang, J. M. Mabry, and A. K. Kota, “Coalescence-induced jumping of droplets on superomniphobic surfaces with macrotextureVahabi, H., Wang, W., Mabry, J. M., & Kota, A. K. (2018). Coalescence-induced jumping of droplets on superomniphobic surfaces with macrotexture, (November), 1–8.,” no. November, pp. 1–8, 2018.

[10] S. Gao, Q. Liao, W. Liu, and Z. Liu, “Coalescence-Induced Jumping of Nanodroplets on Textured Surfaces,” pp. 5–10, 2018.

[11] K. Zhang, Z. Li, M. Maxey, S. Chen, and G. E. Karniadakis, “Self-Cleaning of Hydrophobic Rough Surfaces by Coalescence- Induced Wetting Transition,” 2019.

[12] N. Miljkovic *et al.*, “Jumping-Droplet-Enhanced Condensation on Scalable Superhydrophobic Nanostructured Surfaces,” 2013.

[13] S. Chavan *et al.*, “Heat Transfer through a Condensate Droplet on Hydrophobic and Nanostructured Superhydrophobic Surfaces,” 2016.
[14] K. M. Wisdom, J. A. Watson, X. Qu, F. Liu, G. S. Watson, and C.-H. Chen, “Self-cleaning of superhydrophobic surfaces by self-propelled jumping condensate,” *Proc. Natl. Acad. Sci.*, vol. 110, no. 20, pp. 7992–7997, 2013.
[15] S. Nishimoto and B. Bhushan, “RSC Advances Bioinspired self-cleaning surfaces with,” pp. 671–690, 2013.
[16] Q. Zhang, M. He, J. Chen, J. Wang, and L. Jiang, “Anti-icing surfaces based on enhanced self-propelled jumping of condensed water microdroplets,” pp. 0–6, 2013.
[17] J. Lv, Y. Song, L. Jiang, and J. Wang, “Bio-Inspired Strategies for Anti-Icing,” no. 4, pp. 3152–3169, 2014.
[18] B. Zhang, X. Zhao, and B. Hou, “RSC Advances Fabrication of durable anticorrosion superhydrophobic surfaces on aluminum substrates via a facile one-step electrodeposition,” pp. 35455–35465, 2016.
[19] B. Zhang *et al.*, “Biomimetic one step fabrication of manganese stearate superhydrophobic surface as an efficient barrier against marine corrosion and Chlorella vulgaris -induced biofouling,” *Chem. Eng. J.*, vol. 306, pp. 441–451, 2016.
[20] A. Phys, N. Miljkovic, D. J. Preston, R. Enright, and E. N. Wang, “Jumping-droplet electrostatic energy harvesting Jumping-droplet electrostatic energy harvesting,” vol. 013111, no. June 2014, 2017.
[21] J. Ju, H. Bai, Y. Zheng, T. Zhao, R. Fang, and L. Jiang, “A multi-structural and multi-functional integrated fog collection system in cactus,” *Nat. Commun.*, vol. 3, pp. 1246–1247, 2012.
[22] C. Werner, C. Neinhuis, and C. Werner, “Chem Soc Rev,” vol. 45, no. 2, 2016.
[23] Q. Wang, X. Yao, H. Liu, D. Quéré, and L. Jiang, “Self-removal of condensed water on the legs of water striders,” vol. 112, no. 30, 2015.
[24] P. B. Warren, “Vapor-liquid coexistence in many-body dissipative particle dynamics,” *Phys. Rev. E - Stat. Physics, Plasmas, Fluids, Relat. Interdiscip. Top.*, vol. 68, no. 6, pp. 1–8, 2003.
[25] S. Y. Trofimov, E. L. F. Nies, and M. A. J. Michels, “Thermodynamic consistency in dissipative particle dynamics simulations of strongly nonideal liquids and liquid mixtures,” *J. Chem. Phys.*, vol. 117, no. 20, pp. 9383–9394, 2002.
[26] I. Pagonabarraga and D. Frenkel, “Dissipative particle dynamics for interacting systems,” *J. Chem. Phys.*, vol. 115, no. 11, pp. 5015–5026, 2001.
[27] P. Español and P. B. Warren, “Perspective: Dissipative particle dynamics,” *J. Chem. Phys.*, vol. 146, no. 15, 2017.
[28] A. Ghoufi, J. Emile, and P. Malfreyt, “Recent advances in Many Body Dissipative Particles Dynamics simulations of liquid-vapor interfaces.,” *Eur. Phys. J. E. Soft Matter*, vol. 36, no. 1, p. 10, 2013.
[29] B. Leimkuhler and X. Shang, “On the numerical treatment of dissipative particle dynamics and related systems,” *J. Comput. Phys.*, vol. 280, pp. 72–95, 2015.
[30] A. Boromand, S. Jamali, and J. M. Maia, “Viscosity measurement techniques in Dissipative Particle Dynamics,” *Comput. Phys. Commun.*, vol. 196, pp. 149–160, 2015.
[31] Z. Li, X. Bian, Y. H. Tang, and G. E. Karniadakis, “A dissipative particle dynamics method for arbitrarily complex geometries,” *J. Comput. Phys.*, vol. 355, pp. 534–547, 2018.
[32] M. Arienti, W. Pan, X. Li, and G. Karniadakis, “Many-body dissipative particle dynamics simulation of liquid/vapor and liquid/solid interactions,” *J. Chem. Phys.*, vol. 134, no. 20, 2011.
[33] C. Lan, S. Pal, Z. Li, and Y. Ma, “Numerical Simulations of the Digital Microfluidic Manipulation of Single Microparticles,” *Langmuir*, vol. 31, no. 35, pp. 9636–9645, 2015.
[34] M. Ahmadlouydarab, C. Lan, A. K. Das, and Y. Ma, “Coalescence of sessile microdroplets subject to a wettability gradient on a solid surface,” *Phys. Rev. E*, vol. 94, no. 3, pp. 1–12, 2016.
[35] B.-Y. Cao, M. Chen, and Z.-Y. Guo, “Liquid flow in surface-nanostructured channels studied by molecular dynamics simulation,” *Phys. Rev. E*, vol. 74, no. 6, p. 066311, 2006.
[36] C. Chen *et al.*, “A many-body dissipative particle dynamics study of spontaneous capillary imbibition and drainage,” *Langmuir*, 2010.
[37] C. C. Chang, C. J. Wu, Y. J. Sheng, and H. K. Tsao, “Resisting and pinning of a nanodrop by trenches on a hysteresis-free surface,” *J. Chem. Phys.*, vol. 145, no. 16, 2016.
[38] R. Enright, N. Miljkovic, J. Sprittles, K. Nolan, R. Mitchell, and E. N. Wang, “How coalescing droplets jump,” *ACS Nano*, vol. 8, no. 10, pp. 10352–10362, 2014.
[39] Q. Sheng *et al.*, “How solid surface free energy determines coalescence-induced nanodroplet jumping : A molecular dynamics investigation How solid surface free energy determines coalescence-induced nanodroplet jumping : A molecular dynamics investigation,” vol. 245301, 2017.
[40] U. O. M. Vázquez, W. Shinoda, P. B. Moore, C. C. Chiu, and S. O. Nielsen, “Calculating the surface tension between a flat solid and a liquid: A theoretical and computer simulation study of three topologically different methods,” *J. Math. Chem.*, vol. 45, no. 1, pp. 161–174, 2009.
[41] F. Liu, G. Ghigliotti, and J. J. Feng, “Numerical simulations of self-propelled jumping upon drop coalescence on non-wetting surfaces,” pp. 39–65, 2014.
[42] A. Cavalli *et al.*, “Electrically induced drop detachment and ejection,” *Phys. Fluids*, vol. 28, no. 2, 2016.
[43] M. A. Islam and A. Y. Tong, “A Numerical Study on Electrowetting-Induced Droplet Detachment From Hydrophobic Surface,” *J. Heat Transfer*, vol. 140, no. 5, p. 052003, 2018.